

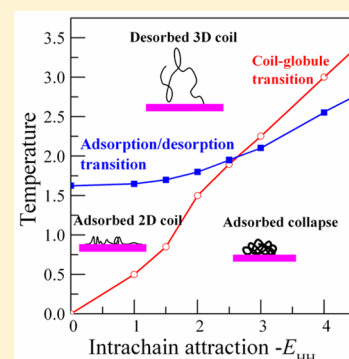
Interplay of Coil–Globule Transition and Surface Adsorption of a Lattice HP Protein Model

Meng-Bo Luo,^{*,†} Jesse D. Ziebarth,[‡] and Yongmei Wang[‡]

[†]Department of Physics, Zhejiang University, Hangzhou 310027, P. R. China

[‡]Department of Chemistry, The University of Memphis, Memphis, Tennessee 38152, United States

ABSTRACT: An end-grafted hydrophobic-polar (HP) model protein chain with alternating H and P monomers is studied to examine interactions between the critical adsorption transition due to surface attraction and the collapse transition due to pairwise attractive H–H interactions. We find that the critical adsorption phenomenon can always be observed; however, the critical adsorption temperature T_{CAP} is influenced by the attractive H–H interactions in some cases. When the collapse temperature T_c is lower than T_{CAP} , the critical adsorption of the HP chain is similar to that of a homopolymer without intrachain attractions and T_{CAP} remains unchanged, whereas the collapse transition is suppressed by the adsorption. In contrast, for cases where T_c is close to or higher than T_{CAP} , T_{CAP} of the HP chain is increased, indicating that a collapsed chain is more easily adsorbed on the surface. The strength of the H–H attraction also influences the statistical size and shape of the polymer, with strong H–H attractions resulting in adsorbed and collapsed chains adopting two-dimensional, circular conformations.



1. INTRODUCTION

Precise control of the adsorption of proteins on solid surfaces is a key to a wide variety of biological and technological applications.^{1–3} Proteins are commonly immobilized on surfaces both in microarrays and other studies of protein function^{4,5} and in the creation of biosensors⁶ and biocatalysts.^{7,8} The success of these applications depends on proteins maintaining their native state and function when adsorbed to the surface and on the prevention of nonspecific protein binding.^{5,9} Protein adsorption also plays an important role in the outcome of biomaterials (e.g., biomedical implants, artificial tissue scaffolds, and nanoparticles for drug delivery) *in vivo*, as proper protein adsorption contributes to cell adhesion and the integration of the biomaterial with the circulatory system, while the adsorption of undesired proteins can contribute to failure due to immune responses or fouling.^{3,10,11} Protein–surface interactions are also relevant to understanding many diseases, as they are the first step in many biological processes, including blood clotting and the formation of protein aggregates, such as the amyloid plaques found in Alzheimer’s disease.^{3,12}

Because of the importance of protein adsorption in these many applications, investigation of the interplay between the folding and adsorption processes and how adsorption impacts protein conformations is highly valuable. Experiments, including a variety of spectroscopic methods, have been able to show that surface adsorption can result in changes in the conformation and thermodynamic stability of a protein and that these changes are dependent on a variety of factors, such as temperature, pH, protein concentration, and the hydrophobicities of the protein and surface.^{2,3,9,10,13} However, experiments have not been able to fully address many aspects of the relationship between protein adsorption and conforma-

tional changes and are complicated by the complex heterogeneity of interactions between real protein chains and surfaces.¹⁴ Therefore, theoretical and computational efforts that often utilize simplified, coarse-grained protein models have been used to supplement experiments and provide a basic understanding of protein adsorption.

One minimalist model used to investigate protein folding and adsorption is the hydrophobic-polar (HP) model, in which protein monomers are modeled on a lattice as either hydrophobic (H) or polar (P) beads.^{15,16} Within the HP model, the many thermodynamic factors underlying complex processes, such as protein folding and adsorption, are reduced to a few basic terms (i.e., enthalpic interactions between chain segments or between the chain and surface and entropically excluded volume interactions). One route through which the HP model can be used to understand protein adsorption and/or folding is the study of two transitions, the coil–globule and the critical adsorption transitions, that are the result of a balance between these thermodynamic terms. The coil–globule or collapse transition is one of the first steps in the protein folding process¹⁷ and occurs when attractive interactions between hydrophobic protein monomers become strong enough to balance the conformational entropy lost by the protein adopting compact globule conformations. A recent experiment using synthetic polymers containing hydrophobic and polar monomers, mimicking HP model chains, confirmed that attractions between hydrophobic monomers are sufficient to be the driving force of the collapse transition.¹⁸ The critical

Received: June 19, 2014

Revised: November 25, 2014

Published: December 2, 2014

adsorption point (CAP) on the other hand marks the transition of a protein which prefers being in solution to being adsorbed on the surface and also involves a balance between entropic and enthalpic effects.^{19–22} The CAP is the point at which a polymer just becomes adsorbed to a surface and occurs when the conformational entropy lost by a polymer chain near a surface is offset by attractive interactions with the surface. Thus, the thermodynamics and potential conformational changes of the process through which a folded protein adsorbs on a surface, for example, can be understood in terms of these two transitions, as some hydrophobic interactions underlying the collapsed conformation of the protein can unravel to allow for additional chain–surface attractive interactions.

Over the last quarter century, the HP and other simple coarse-grained models have been successfully used to provide insight into the conformational changes of proteins and other macromolecules during adsorption both in terms of these transitions and in a variety of other ways. First, the adsorption of HP-like chains with various sequence types on surfaces with various patterns has been studied to understand pattern recognition.^{23,24} These studies have revealed that the adsorption of copolymers on heterogeneous surfaces can proceed via an initial nonspecific adsorption similar to the critical adsorption transition, followed by a reorganization in which the surface pattern is recognized by the copolymer, and that such a two-stage adsorption process depends on the chain sequence, surface pattern, and interaction parameters.^{25–27} Additionally, Moghaddam and Chan investigated the adsorption of block copolymers on patterned surfaces and showed that the sharpness of the adsorption transition was enhanced through the introduction of additional either attractive or repulsive chain–surface interactions.²⁸ However, these studies did not include intrachain interactions and, therefore, could not consider the balance between intrachain and chain–surface interactions that underlies protein adsorption. Second, the adsorption of a homopolymer with intrachain interactions (i.e., basically, a chain consisting of only the H beads of an HP chain) has been considered, and it was shown that the presence of the surface promoted chain collapse and increased the internal structural organization (e.g., helices and antiparallel sheets) in the chain.²⁹ Also, chains with strong intrachain interactions were shown to undergo two types of adsorption transitions: a “docking” transition, in which a collapsed chain does not deform upon adsorption, for weak chain–surface attractions and a “flattening” transition, in which the chain adopts two-dimensional conformations after adsorption for strong chain–surface attractions. Finally, several studies have examined the adsorption of HP chains directly. Rybicka and Sikorski compared the adsorption of several HP sequences with that of a homopolymer containing only H-type beads on a homogeneous surface.³⁰ They showed that the collapse of chains weakly adsorbed on a surface was roughly independent of the chain sequence; however, under strong adsorption, chains underwent a sequence-dependent rearrangement similar to the previously discussed “flattening” transition. Studies of HP chains interacting with surfaces have also confirmed the experimental observation that the presence of the surface can significantly alter the lowest energy conformation of a folded protein^{13,31,32} and have been used to determine conformational pseudophase diagrams of HP chains near a surface that shows how temperature and the strength of attractive interactions impact adsorption and folding.^{14,33,34}

In this work, we seek to increase understanding of the relationship between protein adsorption and conformation change through a systematic examination of the interplay between the collapse and critical adsorption transitions. Specifically, we study the protein folding and adsorption processes by determining the temperatures of collapse, T_c , and critical adsorption, T_{CAP} , transitions for HP chains end-grafted to a solid surface that equally attracts H and P monomers. In contrast with most previous simulations of the adsorption of HP chains that have used a specific short sequence with a well-defined ground state,^{13,31–34} we use a simple alternating HP sequence and vary the chain length from 10 to 400, allowing us to investigate the potential influence of chain length on collapse and adsorption. The current study also investigates the behavior of the chain at more intrachain attraction strengths and over a wider temperature range than was considered in previous studies of the relationship between chain collapse and surface adsorption.^{29,30} We show that, while the critical adsorption point can always be observed and is roughly independent of chain length, T_{CAP} is affected by the presence of intrachain attractions in some cases. Specifically, if $T_c > T_{CAP}$ (i.e., the chain is already collapsed when the adsorption transition is attempted), the critical adsorption transition occurs at a higher temperature than a corresponding homopolymer without intrachain attractions, indicating that collapsed chains are more easily adsorbed. In contrast, if $T_c < T_{CAP}$ (i.e., the chain is already adsorbed when the collapse transition is attempted), T_c is suppressed and it is more difficult to collapse the adsorbed chain than a corresponding chain that is free in solution. Finally, we examine how the strength of the hydrophobic intrachain and chain–surface attractions impact chain conformations.

2. SIMULATION MODEL AND SIMULATION METHOD

Our simulation system is embedded in the three-dimensional (3D) simple cubic (sc) lattice. A self-avoiding walk (SAW) HP protein model with alternate H and P monomers is adopted. Other sequences representing different protein types could have been used;^{13–15,35,36} however, since the current study focuses on the interplay between the two transitions, we focus on a generic alternating HP chain that can be easily extended to long chains. Additionally, we note that both the collapse and adsorption of an alternating HP sequence have been shown to differ from a homopolymer with intrachain attractive interactions.^{30,37} The protein of length N is composed of $N/2$ H monomers and $N/2$ P monomers. Every monomer occupies one lattice site. Bond lengths between monomers fluctuate among 1, $\sqrt{2}$, and $\sqrt{3}$ lattice constants. The bond can be taken from 26 allowed bond vectors obtained from the set $\{(1,0,0), (1,1,0), (1,1,1)\}$ by symmetry operations of the sc lattice. However, bond crossing is not allowed. In this coarse-grained model, the monomers do not correspond to specific atoms in a polymer but rather to small groups of atoms, and the bonds do not represent specific covalent bonds between two atoms but, instead, the linkages between monomers. The simulation box is a cuboid with sizes L_x , L_y , and L_z in the x , y , and z directions, respectively. Periodic boundary conditions are employed in the x and y directions, while the z direction is confined by an infinitely large flat surface located at $z = 0$. The surface is impenetrable to the polymer, so polymer monomers are restricted to lie in the upper half space ($z > 0$). Polymer chain lengths studied are in the range of $N = 10$ to 400. The simulation box is always large enough to ensure no finite size

effects on the simulation results. To this end, the dimensions of the simulation box in all three directions are always larger than the chain length N .

The first monomer, which is always an H, is considered to be adsorbed to the impenetrable surface and is grafted at the center of the $z = 1$ layer. The rest of the chain is first grown using the monomer insertion method.³⁸ Then the chain is subjected to Brownian motion achieved by the dynamic Monte Carlo (MC) technique. Polymer monomers that are located on the $z = 1$ layer are considered to be adsorbed to the surface. An attractive polymer–surface interaction is assigned for all monomers on the $z = 1$ layer next to the surface. A two-dimensional (2D) sketch of our 3D simulation system is presented in Figure 1.

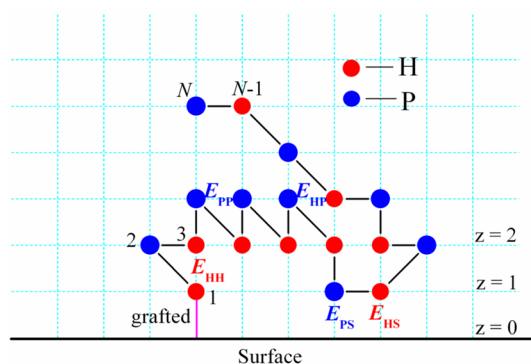


Figure 1. 2D sketch of our 3D simulation model for an end-grafted HP protein model chain. Red and blue ● represent monomers H and P, respectively. Monomers are numbered from 1 to N for a polymer with length N . The first monomer H is grafted to the surface. The nearest neighbor interactions are E_{HH} , E_{HP} , E_{PP} , E_{HS} , and E_{PS} , as shown.

The energy of a conformation is a summation of all nearest-neighbor (NN) contact interactions among the chain and all nearest-neighbor contact interactions between the chain and surface.^{14,15,36} We have

$$E = \sum_{1 \leq i < j \leq N} E_{ij} \delta(r_{ij} - 1) + \sum_i E_{is} \delta(z_i - 1) \quad (1)$$

where r_{ij} is the spatial distance between two nonbonded monomers i and j and z_i is the distance of monomer i away from the surface. The delta function $\delta(x - 1) = 1$ if $x = 1$, and 0 otherwise. The monomer–surface energy depends on two parameters E_{HS} and E_{PS} . It is known that the adsorption of a copolymer chain is influenced by the properties of the surface.²⁸ Here, we consider a surface which attracts both H and P monomers. Therefore, we set $E_{HS} = E_{PS} = -1$. The monomer–monomer energy depends on three parameters E_{HH} , E_{HP} , and E_{PP} . We set $E_{HP} = E_{PP} = 0$, while the value of E_{HH} is negative and varied. Therefore, the energy of polymer can be expressed as¹⁴

$$E = \sum E_{HH} n_{HH} + \sum E_{HS} n_{HS} + \sum E_{PS} n_{PS} \quad (2)$$

where n_{HH} , n_{HS} , and n_{PS} represent the NN contact numbers of H–H, H–surface, and P–surface pairs, respectively. $|E_{HS}|$ is used as the unit of energy while $|E_{HS}|/k_B$ is the unit of temperature, where k_B is the Boltzmann constant. The variable parameters in this work are the H–H interaction E_{HH} and temperature T . Variation in E_{HH} from zero to negative numbers

will allow us to investigate the adsorption of the HP chain on the surface in the absence ($E_{HH} = 0$) or presence of the intrachain hydrophobic interaction.

The Brownian motion of the polymer chain is attributed to local moves of chain monomers. Polymer dynamics is achieved by bond fluctuation,³⁹ similar to that used for one-site and eight-site polymer models on the sc lattice.⁴⁰ For each trial move, a monomer is chosen randomly to move to one of its six NN sites. If the chosen site is already occupied by another monomer, or such a move will violate bond crossing and bond length restriction, the trial move is abandoned. Otherwise, the trial move will be accepted with a probability $p = \min[1, \exp(-\Delta E/k_B T)]$, where ΔE is the energy difference between new and old configurations. It has been pointed out that the Metropolis method may have problems in describing the behavior of HP chains at low temperatures ($k_B T < 0.3|E_{HH}|$) in comparison with the Wang–Landau method.¹⁴ At these low temperatures, the sampling efficiency using the Metropolis algorithm can be poor, as the polymer can become trapped in low-energy states. As we use the Metropolis method in this work, we focus on polymer behavior near T_{CAP} and T_c^0 , which are higher than $0.3|E_{HH}|$. The results of the Metropolis and Wang–Landau methods are very similar for $k_B T > 0.3|E_{HH}|$,¹⁴ and ergodicity can be satisfied by a long simulation run using the Metropolis algorithm.

The chain continuously and gradually changes its spatial configuration by these local motions. The time unit is one Monte Carlo step (MCS) during which $N - 1$ trial moves are attempted since the first monomer is always adsorbed. To avoid correlation between two configurations, we measure the chain's statistical properties only after a regular time interval $\tau = N^{2.13}$ MCS. Typically, each simulation is run as long as 1000τ , and 5000 independent runs are simulated. The results are thus averaged over 5 million independent configuration samples.

We also adopted an annealing process in simulations of chain configuration at different temperatures. Simulations begin at a high temperature with the chain in a desorbed state and in a random coil configuration. Then we slowly decrease the temperature. The temperature decrement step is not a constant but is specially chosen in advance for clearly presenting the collapse and adsorption transitions and for saving calculation time simultaneously. To this end, we first roughly estimate the two transition temperatures using a simulation with a large temperature decrement step and then adopt a small temperature decrement step around the transition temperatures in a second simulation. At each temperature, the system is updated for a total of 1000τ MCS as described above. The final configuration at the previous temperature was used as the initial configuration for the subsequent temperature. Every independent simulation run ends at a low temperature far below the CAP, where the chain is in a deeply adsorbed state.

3. RESULTS AND DISCUSSION

3.1. Coil–Globule Transition in Dilute Solution. We at first determine the collapse transition of the alternating HP model chain in a dilute solution. The chain is annealed from a high to a low temperature. The dependence of the mean square end-to-end distance $\langle R^2 \rangle$ on the temperature T is presented in Figure 2 for the case where $E_{HH} = -1$. The inset shows that the scaling $\langle R^2 \rangle \propto N^{1.2}$ at high temperature changes to $\langle R^2 \rangle \propto N^{0.65}$ at low temperature, indicating a collapse transition from a random coil to a compact sphere. $\langle R^2 \rangle / N$ has the steepest decrease at $T = 0.75$, that is, the temperature at which $d\langle R^2 \rangle /$

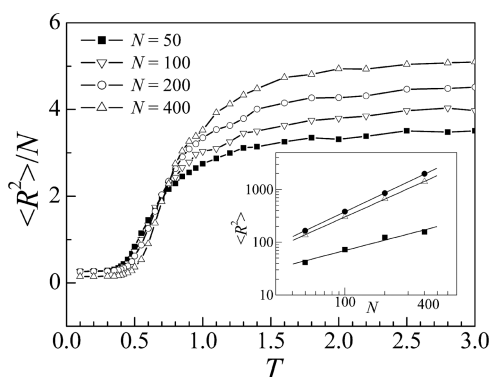


Figure 2. Dependence of mean square end-to-end distance $\langle R^2 \rangle$ on temperature T for the free HP chain with $E_{HH} = -1$ in dilute solution. The inset presents the log–log plot of $\langle R^2 \rangle$ as a function of the chain length N at $T = 2, 1,$ and 0.5 (from top to bottom). The straight lines are the best fits with slopes 1.19, 1.12, and 0.65 for $T = 2, 1,$ and 0.5 , respectively.

dT is at a maximum. $T = 0.75$ is also roughly the crossing point for different chain lengths. Therefore, we identify a coil–globule transition at $T_c^0 = 0.75$ when $E_{HH} = -1$ for the HP chain in dilute solution. Since the temperature T and E_{HH} are interrelated through the Boltzmann factor, a variation in E_{HH} would shift T_c^0 according to $T_c^0 = 0.75|E_{HH}|$ for the HP chain in dilute solution. Here T_c^0 designates the coil–globule transition temperature of the HP chain in the dilute solution in the absence of any surface.

3.2. Adsorption of End-Grafted HP Chain. Next, we simulate the adsorption of the end-grafted HP chain with $E_{HH} = -1$ by annealing the chain with the head H monomer grafted on a flat surface and estimate the collapse transition and the critical adsorption transition temperatures. The critical adsorption transition temperature is estimated from the temperature dependence of the mean surface contact number $\langle M \rangle$ of the chain. $\langle M \rangle$ as a function of chain length at different temperatures is plotted in log–log scales in Figure 3. On the basis of the Eisenriegler, Kremer, and Binder (EKB) scaling theory,¹⁹ the scaling relation $\langle M \rangle \sim N^\phi$ is satisfied at the critical adsorption point T_{CAP} . Meirovitch and Livne have estimated that $T_{CAP} = 3.44 \pm 0.01$ and the crossover exponent $\phi = 0.530 \pm 0.007$ for a SAW chain with fixed bond length ($b = 1$) on the

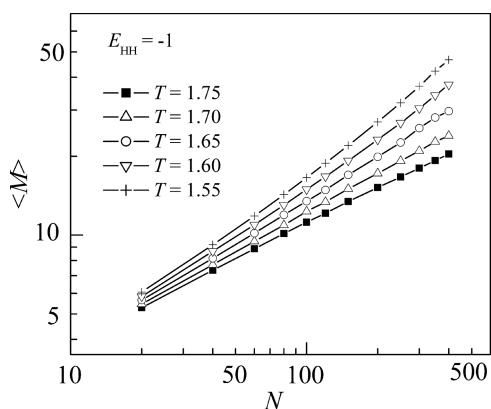


Figure 3. Log–log plot of the surface contact number $\langle M \rangle$ versus chain length N at temperatures $T = 1.55, 1.6, 1.65, 1.7,$ and 1.75 for an HP polymer with $E_{HH} = -1$. The statistical error of each Monte Carlo datum is smaller than the symbol size.

sc lattice with MC simulations.⁴¹ The plot of $\langle M \rangle$ versus chain length N has a concave upward curve at temperatures below T_{CAP} and a convex downward curve at temperatures above T_{CAP} . For the present bond-fluctuation SAW HP model, we estimate $T_{CAP} = 1.65 \pm 0.02$ and $\phi = 0.54 \pm 0.01$. The results are close to that estimated for the adsorption of a bond-fluctuation SAW homopolymer without intrachain attractive interactions, where $T_{CAP} = 1.625$ and $\phi = 0.52$ have been estimated by using a finite-size scaling formula $\langle M \rangle = N^\phi [a_0 + a_1(\epsilon - \epsilon_c)N^{1/\delta} + O((\epsilon - \epsilon_c)^2 N^{2/\delta})]$,^{42,43} indicating that hydrophobic interactions have little effect on T_{CAP} as long as the attractive interactions with the surface are the same for both H and P monomers.

The coil–globule transition temperature for an end-grafted chain is estimated from the temperature dependence of the mean square end-to-end distance $\langle R^2 \rangle$. Figure 4 shows the

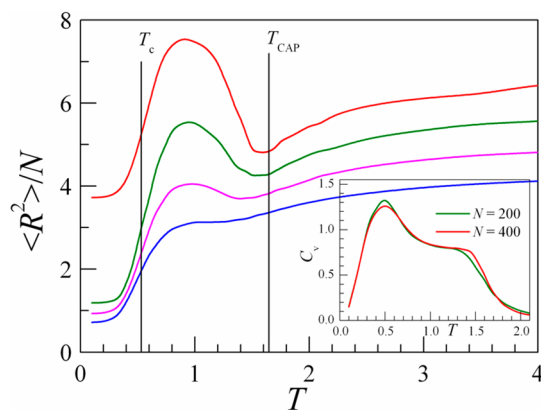


Figure 4. Dependence of mean square end-to-end distance $\langle R^2 \rangle$ on temperature T for the end-grafted HP chain with $E_{HH} = -1$. Chain lengths are $N = 50, 100, 200,$ and 400 from bottom to top. The vertical straight lines show the locations of $T_{CAP} = 1.65$ and $T_c = 0.5$, respectively. The inset presents the heat capacity per monomer for the end-grafted HP chain with $N = 200$ and $N = 400$.

dependence of $\langle R^2 \rangle$ on T for the end-grafted HP polymer with $E_{HH} = -1$. At the critical adsorption temperature $T_{CAP} = 1.65$, we find that $\langle R^2 \rangle$ tends to be a local minimum, which is in agreement with the results of adsorption of a homopolymer chain.⁴³ However, unlike the adsorption of a homogeneous SAW polymer on a surface where the $\langle R^2 \rangle$ increases monotonically as the temperature is lowered below T_{CAP} due to the flattening of the chain on the surface, $\langle R^2 \rangle$ for the end-grafted HP chain increases when T is lowered from T_{CAP} to about $T = 1$ and then decreases afterward. The sharp decrease of $\langle R^2 \rangle$ below $T = 1$ is a result of the coil–globule transition of the chain driven by the intrachain hydrophobic attraction. In contrast to the coil–globule transition of free chains (Figure 2), the plots of $\langle R^2 \rangle/N$ versus T for different chain lengths of end-grafted chains do not cross, and we, therefore, cannot use the crossing point to define the coil–globule transition. We can however still find the steepest decrease of $\langle R^2 \rangle$, which takes place at about $T = 0.5$ and is roughly independent of the chain length. We also find a peak in the heat capacity at $T = 0.5$ for the HP chain as shown in the inset of Figure 4. We therefore identified this temperature as the collapse transition temperature of a surface-absorbed chain $T_c = 0.5$. This $T_c = 0.5$ of the end-grafted HP chain is lower than $T_c^0 = 0.75$ for the free HP chain. We therefore conclude that the collapse transition of the HP polymer is suppressed by being adsorbed to the surface.

When $T_c^0 < T_{CAP}$, the chain undergoes the adsorption transition before the collapse transition can occur. Surface adsorption makes it more difficult for the chain to adopt conformations that provide a sufficient number of H–H contacts for collapse to occur, reducing T_c from its value in a bulk solution. Figure 5 presents the number of H–H contacts

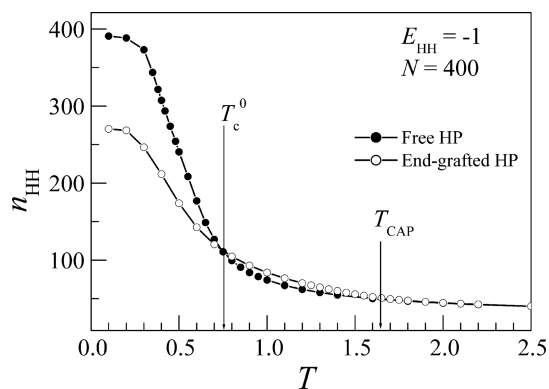


Figure 5. Dependence of the number of H–H contacts, n_{HH} , on the temperature T for HP chains in dilute solution and end-grafted on a surface. The length of the HP chain is $N = 400$, and the H–H interaction $E_{HH} = -1$.

for the HP chains in dilute solution and end-grafted on the surface. Both HP chains have the same H–H interaction $E_{HH} = -1$. Above T_{CAP} of the end-grafted chain, n_{HH} is small and the same for both chains. At temperature $T_c^0 < T < T_{CAP}$, n_{HH} of the end-grafted HP chain is slightly larger than that of the free chain, indicating that the adsorption of the chain promotes the formation of H–H pairs. Below T_c^0 , however, we find that n_{HH} of the end-grafted HP chain is significantly smaller, clearly indicating that surface adsorption prevents the collapse of chain at low temperatures. This reduces T_c for the end-grafted HP chain. On the other hand, the critical adsorption of the polymer is not influenced by the collapse transition of the polymer if $T_c^0 < T_{CAP}$. From the heat capacity, we find a shoulder at higher temperature dependent on the chain length. The temperature at the shoulder is consistent with the CAP, determined from the location of the minimum of $\langle R^2 \rangle$, for the finite chain.

Comparing data in Figures 2 and 4 for $T < T_c$, one can notice that $\langle R^2 \rangle / N$ in Figure 4 increases with N and is much bigger than that of a free HP chain in solution, as shown in Figure 2. The reason is that the adsorbed chain adopts a roughly 2D conformation at $T \ll T_{CAP}$, and the subsequent coil–globule transition driven by the intrachain hydrophobic attraction now occurs within this 2D conformation. As has been previously shown for a homopolymer with intrachain attractions, the collapse of a chain in 2D takes place at a lower temperature than collapse in 3D, since a 2D chain conformation will have less pairwise attraction.²⁹ As will be shown, we find that the adsorbed chain is anisotropic, since its asphericity parameter $\langle A \rangle$ is even bigger than that of an adsorbed HP chain without H–H attraction. Since $T_c \ll T_{CAP}$, the chain at T_c is already trapped in the random coil state achieved at T_{CAP} ; this would probably result in a more anisotropic conformation because the collapse would likely occur at higher density of H monomers.

We next simulate the adsorption of the HP chain with strong H–H attractions ($E_{HH} = -2, -3$, and -4), while the monomer–surface attractions are fixed as $E_{HS} = E_{PS} = -1$. Increasing E_{HH} effectively shifts the coil–globule transition of

the HP chain when free in solution to higher temperatures, following $T_c^0 = 0.75|E_{HH}|$. Therefore, T_c^0 occurs at 1.5, 2.25, and 3 for $E_{HH} = -2, -3$, and -4 , respectively. These conditions allow us to examine the interplay between the transitions when the collapse transition occurs at a higher temperature than the critical adsorption transition ($E_{HH} = -3$ and -4) and when the transitions occur at approximately the same temperature ($E_{HH} = -2$). First, we determine the collapse transition of end-grafted chains when intrachain attractions are stronger than chain–surface attractions ($E_{HH} < E_{HS} = E_{PS}$) and find that T_c is not influenced by the presence of the surface. As shown in Figure 6, a plot of $\langle R^2 \rangle / N$ versus temperature for $E_{HH} = -2$ and

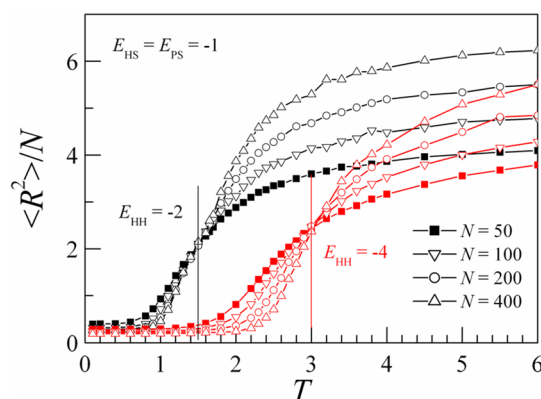


Figure 6. Dependence of mean square end-to-end distance $\langle R^2 \rangle$ on temperature T for the end-grafted HP chain with $E_{HH} = -2$ (black) and -4 (red). The vertical straight lines show the locations of $T_c = 1.5$ for $E_{HH} = -2$ and $T_c = 3.0$ for $E_{HH} = -4$, respectively.

-4 shows the same crossover point as expected for the transition temperature of free chains based on $T_c^0 = 0.75|E_{HH}|$. This behavior is different from the case where $E_{HH} = E_{HS} = E_{PS} = -1$ shown in Figure 4, where the chains with different lengths do not cross over with each other. Although T_c is not influenced by the surface, the conformational size of the chain $\langle R^2 \rangle$ is influenced by the attractive surface, as can be observed through comparison of Figures 2 and 6. We next examine the impact of increasing the strength of intrachain attractions on the critical adsorption transition. Figure 7 presents the surface contact number as a function of chain length at different temperatures for $E_{HH} = -4$. A scaling relation $\langle M \rangle \sim N^{\beta}$ is

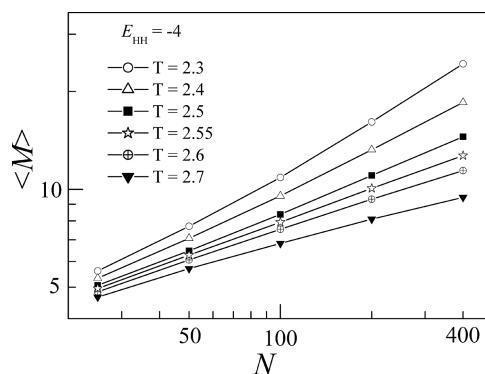


Figure 7. Log–log plot of the surface contact number $\langle M \rangle$ versus chain length N at temperatures $T = 2.3, 2.4, 2.5, 2.55, 2.6$, and 2.7 for an HP polymer with $E_{HH} = -4$. The statistical error of each Monte Carlo datum is smaller than the symbol size.

observed at $T_{\text{CAP}} = 2.55$ with an exponent $\phi = 0.34$. We find that both T_{CAP} and ϕ are different from those of $E_{\text{HH}} = -1$. The results of T_c , T_{CAP} , and ϕ for the HP chains with different intrachain interactions E_{HH} are listed in Table 1. The T_{CAP} for

Table 1. Collapse Transition Temperatures T_c^0 of a Free Chain and T_c of an End-Grafted Chain, the Critical Adsorption Temperature T_{CAP} , and the Crossover Exponent ϕ for Different HP Chains with Different Intrachain Interactions E_{HH} ^a

E_{HH}	T_c^0	T_c	T_{CAP}	ϕ
0	0	0	1.625	0.52
-1	0.75	0.50	1.65	0.54
-2	1.50	1.50	1.80	0.51
-3	2.25	2.25	2.10	0.44
-4	3.00	3.00	2.55	0.34

^aThe polymer–surface interactions $E_{\text{HS}} = E_{\text{PS}} = -1$.

$E_{\text{HH}} = -2, -3,$ and -4 is obviously affected by the collapse of chain when T_c^0 is close to or larger than T_{CAP} of the HP chain with weak H–H interactions. The simulation results show that the presence of intrachain interaction shifts the T_{CAP} to a higher temperature.

At the end of this subsection, we present the phase diagram for the end-grafted HP chain. Figure 8 shows the coil–globule

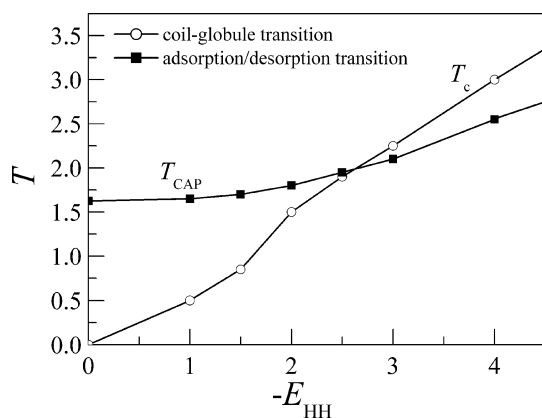


Figure 8. Phase diagram of coil–globule and adsorption transitions for an end-grafted HP chain. The polymer–surface interactions are fixed as $E_{\text{HS}} = E_{\text{PS}} = -1$. Symbols are estimated from simulation, while lines are guides for the eyes.

transition line and the adsorption/desorption transition line for the end-grafted HP chain with polymer–surface interactions $E_{\text{HS}} = E_{\text{PS}} = -1$. There is a specific interaction, named E_{HH}^* , at which the two lines intersect. For intrachain interactions stronger than E_{HH}^* , as temperature decreases, the HP chain changes from a desorbed 3D coil at high temperature to a desorbed collapsed structure at T_c and, finally, to an adsorbed collapse structure at T_{CAP} . For interaction strengths below E_{HH}^* , the HP chain changes from a desorbed 3D coil at high temperature to an adsorbed 2D coil at T_{CAP} and at last to an adsorbed collapse structure below T_c . Here E_{HH}^* is estimated to be about 2.6 times the polymer–surface attraction, and the corresponding temperature is about 2.0.

3.3. Conformational Properties of the End-Grafted HP Chain. To further investigate the interplay between the two transition temperatures, Figure 9a presents the mean surface

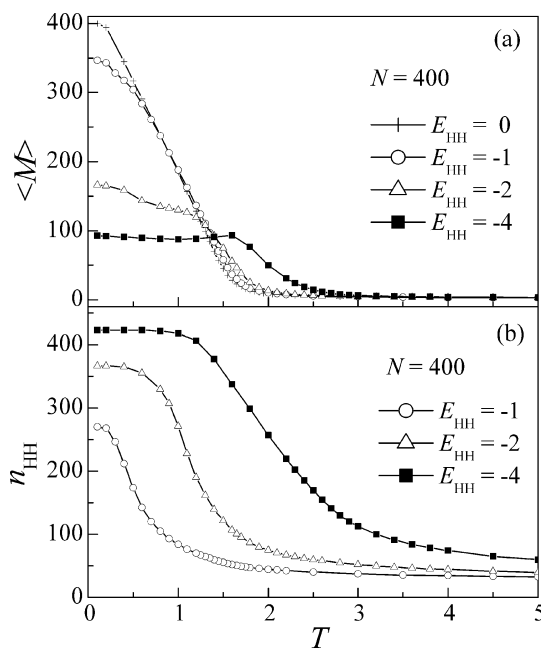


Figure 9. Dependence of (a) mean surface contact number $\langle M \rangle$ and (b) the number of H–H contacts n_{HH} on temperature T for different intrachain interactions E_{HH} . The length of the HP chain is $N = 400$.

contact number $\langle M \rangle$ at different temperatures T for different intrachain interactions E_{HH} . At high temperature $T > T_{\text{CAP}}$, the chain is in a desorbed state with $\langle M \rangle = 0$. At low T , the chain is adsorbed on the surface. One of the ways to observe the T_{CAP} is the substantial increase in $\langle M \rangle$ as T is lowered. At $T = 0$, we have $\langle M \rangle = N$ for the case $E_{\text{HH}} = 0$, indicating that all monomers are adsorbed on the surface, whereas for $E_{\text{HH}} < 0$, $\langle M \rangle$ is less than N due to the collapse of the HP chain, indicating that the conformation of the adsorbed polymer is of a multilayer structure because of the intrachain attraction.^{32,44} The number of H–H contact pairs, n_{HH} , always increases with the decrease of temperature as shown in Figure 9b. Moreover, we find that n_{HH} increases with $|E_{\text{HH}}|$, whereas $\langle M \rangle$ decreases with $|E_{\text{HH}}|$. Similar to behavior that has been observed for homopolymers with intrachain attractions,²⁹ there are less surface contacts but more intrachain contacts as the intrachain attraction increases. This reflects the fact that the adsorbed chain adopts more compact spherical shapes for stronger intrachain interactions.

From Table 1, we find that the crossover exponent ϕ in the scaling relation $\langle M \rangle \sim N^\phi$ is about 0.5 for $T_c < T_{\text{CAP}}$ while it decreases for $T_c > T_{\text{CAP}}$ at strong H–H attraction. For the former case ($T_c < T_{\text{CAP}}$), the conformation of the chain is a random coil near T_{CAP} , and $\langle M \rangle$ behaves similarly near T_{CAP} as shown in Figure 9a, resulting in the same value of the crossover exponent ϕ for $T_c < T_{\text{CAP}}$. For the latter case ($T_c > T_{\text{CAP}}$), the chain is already in a compact globule state at T_{CAP} . The contact number of the compact chain at T_{CAP} is reduced, since the contact monomers are located on the globule surface, as can be observed by comparing data plotted in Figures 3 and 5. For the same reason, the crossover exponent ϕ is reduced for the case $T_c > T_{\text{CAP}}$. We also find that ϕ decreases as $-E_{\text{HH}}$ increases. The reason is that the difference between T_c and T_{CAP} increases with $-E_{\text{HH}}$ as shown in Table 1, and the chain becomes more compact at lower temperature below T_c .

In order to learn more about the conformation of the chain, we have monitored the mean square end-to-end distance $\langle R^2 \rangle$

and its two components parallel to the surface $\langle R^2 \rangle_{xy}$ and normal to the surface $\langle R^2 \rangle_z$ at different internal interactions E_{HH} , as shown in Figure 10. Different behaviors are exhibited

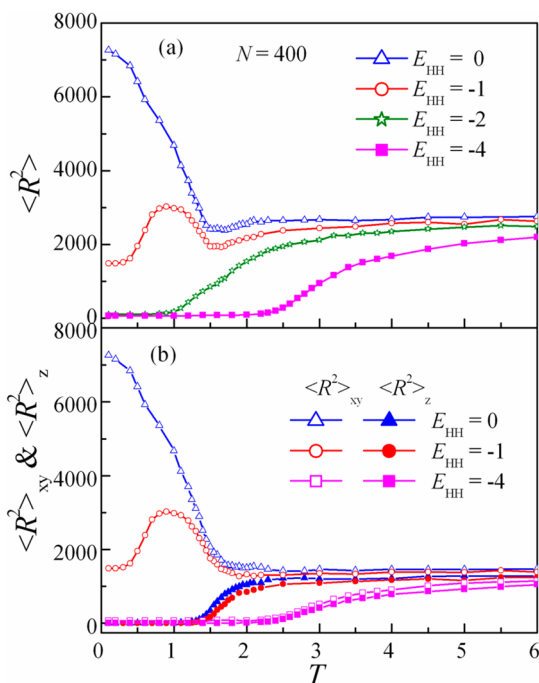


Figure 10. Dependence of (a) the mean square end-to-end distance $\langle R^2 \rangle$ and (b) its components parallel and normal to the surface, $\langle R^2 \rangle_{xy}$ and $\langle R^2 \rangle_z$, respectively, as a function of temperature T for HP polymers with different H–H interactions. The length of the HP chain is $N = 400$.

for three different cases: (1) a chain with no collapse transition when $E_{HH} = 0$, (2) $T_c^0 < T_{CAP}$ with $E_{HH} = -1$, and (3) $T_c^0 \geq T_{CAP}$ with $E_{HH} = -2$ and -4 . For the first case in the absence of intrachain interaction, a slight minimum in $\langle R^2 \rangle$ is found at T_{CAP} that is a result of two changes, as a sharp decrease in $\langle R^2 \rangle_z$ is partially offset by a sharp increase in $\langle R^2 \rangle_{xy}$. As the temperature is further reduced, the increase in $\langle R^2 \rangle_{xy}$ outcompetes the decrease in $\langle R^2 \rangle_z$, resulting in an overall increase in $\langle R^2 \rangle$. The behavior of $\langle R^2 \rangle$ is similar to an earlier finding by exact enumeration of all configurations for a short homogeneous SAW chain.²⁹ For the second case where $T_c^0 < T_{CAP}$, $\langle R^2 \rangle$ first increases as the temperature is lowered just as in the previous case but then $\langle R^2 \rangle$ decreases because of the collapse of the chain. In this second scenario, $\langle R^2 \rangle$ exhibits a maximum at a temperature close to T_c , a distinct feature absent in the other cases. The maximum is also presented in the plot of $\langle R^2 \rangle_{xy}$ as a function of temperature. For the third case where $T_c^0 \geq T_{CAP}$, we find that $\langle R^2 \rangle$, $\langle R^2 \rangle_{xy}$, and $\langle R^2 \rangle_z$ all decrease monotonically with the decrease of T . The chain is already in a compact state at T_{CAP} ; therefore, it deforms little when it adsorbs on a surface, similar to the “docking” transition for a compact chain adsorbed on a weak attractive surface.²⁹

We further calculate the mean asphericity parameter $\langle A \rangle$ of the HP chain. $\langle A \rangle$ is defined as

$$\langle A \rangle = \left\langle \sum_{i>j}^3 (L_i^2 - L_j^2)^2 / 2 \left(\sum_{i=1}^3 L_i^2 \right)^2 \right\rangle \quad (3)$$

in 3D space.⁴⁵ Here L_1^2 , L_2^2 , and L_3^2 are three eigenvalues of the radius of gyration tensor

$$S = \frac{1}{N} \sum_{i=1}^N s_i s_i^T = \begin{pmatrix} S_{xx} & S_{xy} & S_{xz} \\ S_{xy} & S_{yy} & S_{yz} \\ S_{xz} & S_{yz} & S_{zz} \end{pmatrix} \quad (4)$$

where $s_i = \text{col}(x_i, y_i, z_i)$ is the position of monomer i of polymer in a frame of reference with its origin at the center of mass. The asphericity parameter $\langle A \rangle$ ranges from zero for 3D spherically symmetric chain conformations, 0.25 for 2D circular shapes, and one for rod-shaped. It was found that $\langle A \rangle \approx 0.391$ for a linear RW chain and $\langle A \rangle \approx 0.431$ for a linear SAW chain.⁴⁵ Values $\langle A \rangle$ of the HP chain in dilute solution (i.e., free HP chain) and the end-grafted HP chain are calculated. The dependence of $\langle A \rangle$ on temperature T is presented in Figure 11 for the end-grafted HP chains with different intrachain H–H interactions.

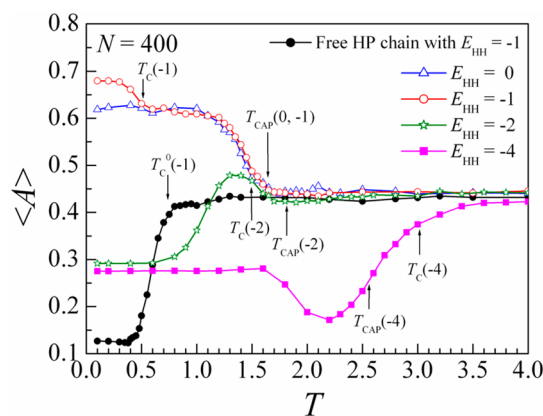


Figure 11. Plot of the asphericity parameter $\langle A \rangle$ vs temperature T for free HP chains with $E_{HH} = -1$ and end-grafted HP chains with different H–H interactions. The HP chain length is $N = 400$. The arrows indicate the location of T_c and T_{CAP} , and the value in parentheses is E_{HH} .

For the free HP chain with $E_{HH} = -1$, $\langle A \rangle$ is about 0.44 at $T \gg T_c$ and decreases steeply at $T_c^0 = 0.75$. $\langle A \rangle$ is about 0.12 at low temperatures ($T < T_c$), clearly showing that the chain is roughly a sphere at temperatures below T_c . For the end-grafted HP chain, the behavior of $\langle A \rangle$, like that of size $\langle R^2 \rangle$, is dependent on the intrachain attraction E_{HH} . Moreover, the behavior of $\langle A \rangle$ is quite complicated due to the competition between T_c and T_{CAP} in the HP chain. For $E_{HH} = 0$, $\langle A \rangle$ increases at T_{CAP} due to the transition from a 3D random coil to a 2D random coil. For $E_{HH} = -1$, $\langle A \rangle$ first increases at $T_{CAP} = 1.65$ and has a second increment at $T_c = 0.5$. The collapse at $T_c \ll T_{CAP}$ happens locally and makes the chain configuration more aspherical. For the case with $E_{HH} = -2$ where T_c is close to T_{CAP} , we find that $\langle A \rangle$ begins to increase when the temperature drops below T_{CAP} and continues to increase at T_c . But, as temperature continues to decrease further below T_c , we find that $\langle A \rangle$ begins to decrease due to the strong collapse of chain as $|E_{HH}| > |E_{HS}|$. For $E_{HH} = -4$, $\langle A \rangle$ decreases at T_c because of collapse and then increases at T_{CAP} because of adsorption; finally, $\langle A \rangle$ plateaus as the chain becomes frozen at low temperatures. From these four behaviors, we conclude that adsorption of the chain increases $\langle A \rangle$, whereas the effect of

collapse is dependent on the strength of intrachain H–H attraction.

If the intrachain H–H attraction is weak where we have $T_c \ll T_{CAP}$, the adsorption of the chain increases ($\langle A \rangle$) and the adsorbed configuration is a random coil. For this case, the collapse at low temperature will induce extra anisotropy and increase $\langle A \rangle$. If the intrachain H–H attraction is moderate where we have $T_c \sim T_{CAP}$, $\langle A \rangle$ is increased due to the adsorption as well as collapse of the chain but will decrease at low temperatures below T_c . Finally, if the intrachain H–H attraction is strong where we have $T_c > T_{CAP}$, $\langle A \rangle$ first decreases due to the collapse and then increases due to the adsorption of the chain. Moreover, for the last two cases, $\langle A \rangle$ at low temperature reaches a plateau with a value close to 0.25, indicating that the adsorbed configuration is roughly a 2D circle.

4. CONCLUSION

We have studied the interplay between the critical adsorption of a lattice HP protein with alternating H and P monomers and the coil–globule transition with the dynamical Monte Carlo method. Simulations are carried out in the simple cubic lattice where bond length can be fluctuated among 1, $\sqrt{2}$, and $\sqrt{3}$ lattice units. We find that the critical adsorption temperature T_{CAP} is influenced by the presence of intrachain attractions responsible for the collapse transition of the polymer. If the coil–globule transition T_c^0 is lower than T_{CAP} then T_{CAP} for the HP polymer is roughly the same as that of a homopolymer without monomer–monomer attractions, but the coil–globule transition T_c is suppressed by adsorption. It is therefore more difficult for a surface adsorbed HP polymer chain to go through the coil–globule collapse than one that is free in solution. On the other hand, if the intrinsic coil–globule transition temperature T_c^0 is higher than T_{CAP} , the T_{CAP} for the HP polymer occurs at a higher temperature than a homopolymer without monomer–monomer attraction; that is, a collapsed chain can be more easily adsorbed. The conformational properties of the end-grafted HP chain are strongly influenced by the pairwise H–H attraction.

There are some limitations in our current simulation model. First, the HP model itself is limited in that it does not consider several factors, such as desolvation effects, that have been shown to be relevant to the behavior of real proteins, such as the cooperativity observed during the folding of many proteins.^{46,47} Second, the sequence we have studied is the HP polymer with a fully alternating sequence in which the surface interactions of H and P monomers are treated as the same. This is a significant simplification and probably does not represent the real experimental situation very well. In most applications, the surface is hydrophilic or hydrophobic. In either case, the surface interactions of H and P monomers would be different. A further extension of our study is to treat the surface interactions of H and P monomers differently. However, the overall conclusion about the mutual impact on the coil–globule transition and the critical adsorption transition would probably still be valid.

AUTHOR INFORMATION

Corresponding Author

*E-mail: luomengbo@zju.edu.cn.

Notes

The authors declare no competing financial interest.

ACKNOWLEDGMENTS

This work was supported by the National Natural Science Foundation of China under Grants 11374255 and 21174132. The U.S. investigators acknowledge partial financial support from the NIH through NIGMS (Grant 1R15GM106326-01A).

REFERENCES

- (1) Nakanishi, K.; Sakiyama, T.; Imamura, K. On the Adsorption of Proteins on Solid Surfaces, a Common but very Complicated Phenomenon. *J. Biosci. Bioeng.* **2001**, *91*, 233–244.
- (2) Gray, J. J. The Interaction of Proteins with Solid Surfaces. *Curr. Opin. Struct. Biol.* **2004**, *14*, 110–115.
- (3) Rabe, M.; Verdes, D.; Seeger, S. Understanding Protein Adsorption Phenomena at Solid Surfaces. *Adv. Colloid Interface Sci.* **2011**, *162*, 87–106.
- (4) Phizicky, E.; Bastiaens, P. I. H.; Zhu, H.; Snyder, M.; Fields, S. Protein Analysis on a Proteomic Scale. *Nature (London)* **2003**, *422*, 208–215.
- (5) Rusmini, F.; Zhong, Z.; Feijen, J. Protein Immobilization Strategies for Protein Biochips. *Biomacromolecules* **2007**, *8*, 1775–1789.
- (6) Besteman, K.; Lee, J. O.; Wiertz, F. G. M.; Heering, H. A.; Dekker, C. Enzyme-Coated Carbon Nanotubes as Single-Molecule Biosensors. *Nano Lett.* **2003**, *3*, 727–730.
- (7) Mateo, C.; Palomo, J. M.; Fernandez-Lorente, G.; Guisan, J. M.; Fernandez-Lafuente, R. Improvement of Enzyme Activity, Stability and Selectivity via Immobilization Techniques. *Enzyme Microb. Technol.* **2007**, *40*, 1451–1463.
- (8) Zhou, Z.; Hartmann, M. Progress in Enzyme Immobilization in Ordered Mesoporous Materials and Related Applications. *Chem. Soc. Rev.* **2013**, *42*, 3894–3912.
- (9) Secundo, F. Conformational Changes of Enzymes upon Immobilization. *Chem. Soc. Rev.* **2013**, *42*, 6250–6261.
- (10) Roach, P.; Eglin, D.; Rohde, K.; Perry, C. C. Modern Biomaterials: A Review—Bulk Properties and Implications of Surface Modifications. *J. Mater. Sci.: Mater. Med.* **2007**, *18*, 1263–1277.
- (11) Mahon, E.; Salvati, A.; Bombelli, F. B.; Lynch, I.; Dawson, K. A. Designing the Nanoparticle–Biomolecule Interface for “Targeting and Therapeutic Delivery”. *J. Controlled Release* **2012**, *161*, 164–174.
- (12) Morriss-Andrews, A.; Bellesia, G.; Shea, J. E. Effects of Surface Interactions on Peptide Aggregate Morphology. *J. Chem. Phys.* **2011**, *135*, 085102.
- (13) Sharma, S.; Berne, B. J.; Kumar, S. K. Thermal and Structural Stability of Adsorbed Proteins. *Biophys. J.* **2010**, *99*, 1157–1165.
- (14) Li, Y. W.; Wüst, T.; Landau, D. P. Generic Folding and Transition Hierarchies for Surface Adsorption of Hydrophobic-Polar Lattice Model Proteins. *Phys. Rev. E* **2013**, *87*, 012706.
- (15) Lau, K. F.; Dill, K. A. A Lattice Statistical Mechanics Model of the Conformational and Sequence Spaces of Proteins. *Macromolecules* **1989**, *22*, 3986–3997.
- (16) Yue, K.; Dill, K. A. Forces of Tertiary Structural Organization in Globular Proteins. *Proc. Natl. Acad. Sci. U.S.A.* **1995**, *92*, 146–150.
- (17) Kuwajima, K. The Molten Globule State as a Clue for Understanding the Folding and Cooperativity of Globular-Protein Structure. *Proteins: Struct. Funct. Genet.* **1989**, *6*, 87–103.
- (18) Murnen, H. K.; Khokhlov, A. R.; Khalatur, P. G.; Segalman, R. A.; Zuckermann, R. N. Impact of Hydrophobic Sequence Patterning on the Coil-to-Globule Transition of Protein-like Polymers. *Macromolecules* **2012**, *45*, 5229–5236.
- (19) Eisenriegler, E.; Kremer, K.; Binder, K. Adsorption of Polymer Chains at Surfaces: Scaling and Monte Carlo Analyses. *J. Chem. Phys.* **1982**, *77*, 6296–6320.
- (20) Hammersley, J. M.; Torrie, G. M.; Whittington, S. G. Self-Avoiding Walks Interacting with a Surface. *J. Phys. A: Math. Gen.* **1982**, *15*, 539–571.
- (21) Gong, Y. C.; Wang, Y. M. Partitioning of Polymers into Pores near the Critical Adsorption Point. *Macromolecules* **2002**, *35*, 7492–7498.

- (22) Descas, R.; Sommer, J.-U.; Blumen, A. Static and Dynamic Properties of Tethered Chains at Adsorbing Surfaces: A Monte Carlo Study. *J. Chem. Phys.* **2004**, *120*, 8831–8840.
- (23) Muthukumar, M. Pattern Recognition in Self Assembly. *Curr. Opin. Colloid Interface Sci.* **1998**, *3*, 48–54.
- (24) Golumbfskie, A. J.; Pande, V. S.; Chakraborty, A. K. Simulation of Biomimetic Recognition between Polymers and Surfaces. *Proc. Natl. Acad. Sci. U.S.A.* **1999**, *96*, 11707–11712.
- (25) Sumithra, K.; Straube, E. Adsorption of Diblock Copolymers on Stripe-Patterned Surfaces. *J. Chem. Phys.* **2006**, *125*, 154701.
- (26) Sumithra, K. The Influence of Adsorbate-Surface Interaction Energy on Adsorption and Recognition of Diblock Copolymers on Patterned Surfaces. *J. Chem. Phys.* **2009**, *130*, 194903.
- (27) Sumithra, K.; Brandau, M.; Straube, E. Adsorption and Pinning of Multiblock Copolymers on Chemically Heterogeneous Patterned Surfaces. *J. Chem. Phys.* **2009**, *130*, 234901.
- (28) Moghaddam, M. S.; Chan, H. S. Selective Adsorption of Block Copolymers on Patterned Surfaces. *J. Chem. Phys.* **2006**, *125*, 164909.
- (29) Chan, H. S.; Wattenbarger, M. R.; Evans, D. F.; Bloomfield, V. A.; Dill, K. A. Enhanced Structure in Polymers at Interfaces. *J. Chem. Phys.* **1991**, *94*, 8542–8557.
- (30) Rybicka, J.; Sikorski, A. Adsorption of Copolymers on Solid Surfaces. *Macromol. Theory Simul.* **2010**, *19*, 135–141.
- (31) Castells, V.; Van Tassel, P. R. Conformational Transition Free Energy Profiles of an Adsorbed, Lattice Model Protein by Multicanonical Monte Carlo Simulation. *J. Chem. Phys.* **2005**, *122*, 084707.
- (32) Radhakrishna, M.; Sharma, S.; Kumar, S. K. Enhanced Wang Landau Sampling of Adsorbed Protein Conformations. *J. Chem. Phys.* **2012**, *136*, 114114.
- (33) Bachmann, M.; Janke, W. Substrate Specificity of Peptide Adsorption: A Model Study. *Phys. Rev. E* **2006**, *73*, 020901R.
- (34) Swetnam, A. D.; Allen, M. P. Improved Simulations of Lattice Peptide Adsorption. *Phys. Chem. Chem. Phys.* **2009**, *11*, 2046–2055.
- (35) Shakhnovich, E. I. Proteins with Selected Sequences Fold into Unique Native Conformation. *Phys. Rev. Lett.* **1994**, *72*, 3907–3910.
- (36) Bachmann, M.; Janke, W. Thermodynamics of Lattice Heteropolymers. *J. Chem. Phys.* **2004**, *120*, 6779–6791.
- (37) Kolinski, A.; Madziar, P. Collapse Transitions in Protein-Like Lattice Polymers: The Effect of Sequence Patterns. *Biopolymers* **1997**, *42*, 537–548.
- (38) Frenkel, D.; Smit, B. *Understanding Molecular Simulations: From Algorithms to Applications*; Academic Press: San Diego, CA, 2002.
- (39) Qian, H.; Sun, L. Z.; Luo, M. B. Simulation Study on the Translocation of a Partially Charged Polymer through a Nanopore. *J. Chem. Phys.* **2012**, *137*, 034903.
- (40) Carmesin, I.; Kremer, K. The Bond Fluctuation Method: A New Effective Algorithm for the Dynamics of Polymers in All Spatial Dimensions. *Macromolecules* **1988**, *21*, 2819–2823.
- (41) Meirovitch, H.; Livne, S. Computer Simulation of Long Polymers Adsorbed on a Surface. II. Critical Behavior of a Single Self-Avoiding Walk. *J. Chem. Phys.* **1988**, *88*, 4507–4515.
- (42) Luo, M. B. The Critical Adsorption Point of Self-Avoiding Walks: A Finite-Size Scaling Approach. *J. Chem. Phys.* **2008**, *128*, 044912.
- (43) Li, H.; Qian, C. J.; Luo, M. B. Simulation of a Flexible Polymer Tethered to a Flat Adsorbing Surface. *J. Appl. Polym. Sci.* **2012**, *124*, 282–287.
- (44) Möddel, M.; Janke, W.; Bachmann, M. Comparison of the Adsorption Transition for Grafted and Nongrafted Polymers. *Macromolecules* **2011**, *44*, 9013–9019.
- (45) Bishop, M.; Saltiel, C. J. Polymer Shapes in Two, Four, and Five Dimensions. *J. Chem. Phys.* **1988**, *88*, 3976–3980.
- (46) Chan, H. S.; Zhang, Z.; Wallin, S.; Liu, Z. Cooperativity, Local-Nonlocal Coupling, and Nonnative Interactions: Principles of Protein Folding from Coarse-Grained Models. *Annu. Rev. Phys. Chem.* **2011**, *62*, 301–326.
- (47) Chan, H. S. Modeling Protein Density of States: Additive Hydrophobic Effects are Insufficient for Calorimetric Two-State Cooperativity. *Proteins: Struct. Funct. Genet.* **2000**, *40*, 543–571.